

## Ultra-fast calorimetry study of $\text{Ge}_2\text{Sb}_2\text{Te}_5$ crystallization between dielectric layers

J. Orava, A. L. Greer<sup>\*</sup>, B. Gholipour, D. W. Hewak, and C. E. Smith

Citation: *Appl. Phys. Lett.* **101**, 091906 (2012); doi: 10.1063/1.4748881

View online: <http://dx.doi.org/10.1063/1.4748881>

View Table of Contents: <http://aip.scitation.org/toc/apl/101/9>

Published by the [American Institute of Physics](#)

---

---



**FIND THE NEEDLE IN THE  
HIRING HAYSTACK**

POST JOBS AND REACH THOUSANDS OF  
QUALIFIED SCIENTISTS EACH MONTH.

PHYSICS TODAY | JOBS  
[WWW.PHYSICSTODAY.ORG/JOBS](http://WWW.PHYSICSTODAY.ORG/JOBS)

## Ultra-fast calorimetry study of $\text{Ge}_2\text{Sb}_2\text{Te}_5$ crystallization between dielectric layers

J. Orava,<sup>1</sup> A. L. Greer,<sup>1,a)</sup> B. Gholipour,<sup>2</sup> D. W. Hewak,<sup>2</sup> and C. E. Smith<sup>3</sup>

<sup>1</sup>*Department of Materials Science and Metallurgy, University of Cambridge, Pembroke Street, Cambridge CB2 3QZ, United Kingdom*

<sup>2</sup>*Optoelectronics Research Centre, University of Southampton, Southampton SO17 1BJ, United Kingdom*

<sup>3</sup>*Mettler-Toledo Ltd., Beaumont Leys, Leicester LE4 1AW, United Kingdom*

(Received 24 April 2012; accepted 16 August 2012; published online 28 August 2012)

Phase changes in chalcogenides such as  $\text{Ge}_2\text{Sb}_2\text{Te}_5$  can be exploited in non-volatile random-access memory, with fast crystallization crucial for device operation. Ultra-fast differential scanning calorimetry, heating at rates up to  $40\,000\text{ K s}^{-1}$ , has been used to study the crystallization of amorphous  $\text{Ge}_2\text{Sb}_2\text{Te}_5$  with and without sandwich layers of  $\text{ZnS-SiO}_2$ . At heating rates up to  $1000\text{ K s}^{-1}$ , the sandwich layers retard crystallization, an effect attributed to crystallization-induced stress. At greater heating rates ( $\geq 5000\text{ K s}^{-1}$ ), and consequently higher crystallization temperatures, the stress is relaxed, and sandwich layers catalyze crystallization. Implications for memory-device performance are discussed. © 2012 American Institute of Physics.

[<http://dx.doi.org/10.1063/1.4748881>]

The chalcogenide  $\text{Ge}_2\text{Sb}_2\text{Te}_5$  (GST) is among the most widely exploited and studied phase-change materials of interest for non-volatile data storage.<sup>1</sup> Thin films of chalcogenides exemplified by GST can be reversibly switched between amorphous and crystalline states. The crystalline state is melted by a short heat pulse and is then rapidly quenched into the amorphous state; less intense heating induces crystallization of the amorphous state. In optical disks (CD-RW, DVD-RW, Blu-ray™), the heating is by laser and the data marks are read using changes in optical reflectance. In phase-change random-access memory (PC-RAM), the heating is by electrical pulse and the state of the memory cells is detected through their resistance. The amorphous state of the chalcogenide has significantly lower reflectance and electrical conductivity than the crystalline state. The present work is motivated by the current interest in chalcogenide-based PC-RAM for non-volatile memory.<sup>2,3</sup>

For this application, crystallization must be rapid, preferably taking less than the 10 ns switching time typical for DRAM.<sup>3</sup> Yet, in a possibly contradictory requirement,<sup>3</sup> under ambient conditions crystallization must be suppressed to permit long-term (>10 yr) data retention. Thus, the temperature dependence of crystallization kinetics is critical in materials selection for PC memory.<sup>4</sup> The crystallization of GST has mostly been studied close to its glass-transition temperature  $T_g$ , when slow rates permit careful characterization. Transmission electron microscopy (TEM),<sup>5,6</sup> atomic-force microscopy,<sup>7</sup> and atomistic modeling<sup>8</sup> have been used to determine incubation times, nucleation rates, and growth rates, all of which are temperature-dependent. The activation energy  $E_a$  for crystallization can be determined by measuring the increase in crystallization temperature  $T_p$  (for example, the temperature of exothermic peaks in DSC) as the heating rate  $\Phi$  is increased. This Kissinger method<sup>9</sup> has been applied not only to DSC<sup>10,11</sup> but also to electrical resistometry<sup>12,13</sup>

and optical measurements.<sup>14</sup> Such studies have contributed to understanding the distinction between materials in which the crystallization is *nucleation-driven* (e.g., GST) or *growth-driven* (e.g., Ag-In-Sb-Te).<sup>15</sup> They may be relevant for studies of data retention, but with crystallization studied only over narrow ranges of  $\Phi$  ( $0.008\text{ K s}^{-1}$  to  $6.7\text{ K s}^{-1}$ ) and  $T_p$  (411 K to 443 K), the times are as much as  $10^9\times$  longer than relevant for PC-RAM switching.

Recent work<sup>16</sup> has applied ultra-fast DSC to as-deposited amorphous a-GST. Heating rates up to  $4\times 10^4\text{ K s}^{-1}$  allow the crystallization to be characterized over a much wider temperature range, up to 650 K, and therefore close to the estimated maximum in crystal growth rate. The temperature dependence of the crystallization rate was taken to be dominated by the temperature dependence of the growth rate, and in this way, the kinetic coefficient for crystal growth  $U_{\text{kin}}$  (the limiting growth velocity when the thermodynamic factor is one) was determined.<sup>16</sup> This has a non-Arrhenius temperature dependence, indicating a high kinetic fragility of the liquid ( $m\approx 90$ ).<sup>16</sup> Furthermore, consistent with the results of Ediger *et al.*<sup>17</sup> on oxide and organic liquids, there was evidence for decoupling of crystal growth from viscous flow on cooling towards  $T_g$ : the growth rate extrapolated to  $T_g$  was found to be  $10^5$  times faster than would be calculated from the viscosity of  $10^{12}\text{ Pa s}$  at the glass transition. As in many previous studies of GST, the ultra-fast DSC was on uncapped thin films, yet it is known that crystallization can be strongly affected by contact with neighboring layers (in sandwich structures, or with a capping or protective layer on top). The present work aims to extend the earlier ultra-fast DSC study to characterize and understand the effects of sandwiching the GST between layers, in this case of  $\text{ZnS-SiO}_2$  (80:20 mol. %).

This material is the usual choice for the dielectric layers that sandwich the chalcogenide thin film in optical disks. These layers optimize performance and, in particular, can increase the number of possible overwrite cycles.<sup>18,19</sup> Ohshima<sup>18</sup> showed that the choice of dielectric layers used

<sup>a)</sup> Author to whom correspondence should be addressed. Electronic mail: [alg13@cam.ac.uk](mailto:alg13@cam.ac.uk).

to sandwich a 30 nm a-GST film can strongly influence the crystallization of the film. Sandwiching between dielectric layers always increased  $T_p$  and  $E_a$ . Later studies, monitoring crystallization by electrical resistometry,<sup>12</sup> DSC,<sup>13</sup> optical measurements,<sup>14,20</sup> x-ray diffraction,<sup>21</sup> and EXAFS and ellipsometry,<sup>22</sup> have confirmed that sandwiching or capping of as-deposited amorphous films of GST impedes their crystallization, as revealed by increased  $T_p$  and  $E_a$ , and by increased incubation and crystallization time on isothermal treatments. An analogous effect of contact with a dielectric is found in the increased  $E_a$  for GST in composite films incorporating TaO<sub>x</sub>.<sup>23</sup>

These studies have used GST films with thickness from 250 nm down to 2 nm. In general, the impeding effect of the sandwich or capping layers is greater, the thinner the GST film. The effect is already detectable at thicknesses as great as 80 nm; for example, at this thickness,  $E_a$  increases from  $2.24 \pm 0.01$  eV for uncapped films to  $2.7 \pm 0.2$  eV for films capped with 4.5 nm of ZnS-SiO<sub>2</sub>.<sup>12</sup> There is practical importance, as the complete erasure time (CET) of the GST film in optical disks increases rapidly with decreasing film thickness.<sup>15</sup> Isothermal crystallization of GST, analyzed according to Johnson-Mehl-Avrami-Kolmogorov (JMAK) kinetics,<sup>13,18</sup> shows the Avrami exponent decreasing with decreasing film thickness, consistent with a reduced dimensionality of crystal growth that has been modeled.<sup>24</sup>

Crystallization of GST is strongly impeded, indicated by an exponential increase in  $T_p$ , with decreasing thickness below 10 nm.<sup>13,20,21</sup> As reviewed in Ref. 25, such an increase in  $T_p$  in thin films is seen in many systems, including a-Si in a-Si/a-SiO<sub>2</sub> superlattices.<sup>26</sup> The crystal nucleation in that case has been modeled assuming, as in Ref. 24, that it occurs in the middle plane of the film.<sup>27</sup> As the critical nucleus is more confined by the sandwich layers of oxide, the effective interfacial energy between the crystal and the amorphous matrix increases due to screening effects from the oxide. The screening length was found to be 0.64 nm, so the strongest effect, ultimately prohibiting any crystal nucleation, is only for the very thinnest amorphous films.<sup>27</sup>

It is notable that the increase in  $T_p$  of a-Si in a-Si/a-SiO<sub>2</sub> superlattices is closely correlated with increasing inhomogeneous strain in the growing crystals,<sup>26,27</sup> suggesting effects of stress. For chalcogenides, including GST, wafer-curvature measurements show that crystallization leads to a build-up of stress, scaling with the volume shrinkage on crystallization.<sup>19</sup> For these uncapped films, the final stress is, however, only about 9% of the value expected for purely elastic deformation, indicating substantial stress relaxation through flow of the amorphous phase. In films of GST sandwiched between 5 nm layers of ZnS-SiO<sub>2</sub>, (80:20 mol. %), stresses are roughly doubled, indicating that the stress relaxation is reduced by capping, perhaps by suppression of creep mediated by surface diffusion.<sup>28</sup> Stresses are higher (relaxation is further impeded) in thinner films,<sup>28</sup> while further heating leads to reduced stress.<sup>19</sup>

As noted by others,<sup>12,21</sup> further study is required to understand the effects of sandwich and capping layers on crystallization. Effects of interface morphology<sup>18</sup> and inter-diffusion<sup>22</sup> have been ruled out. It is of particular interest to understand how crystallization can be inhibited even in

rather thick ( $>10$  nm) layers when screening effects, discussed above,<sup>27</sup> should not have any effect. For these thicker layers, it is important to probe the role of crystallization-induced stress. Ultra-fast DSC opens up the possibility of doing so over a much wider range of temperature than has been possible so far.

Deposition onto pre-cleaned glass microscope slides was by RF sputtering (Nano 38 system, Kurt J. Lesker) at a power of 45 W. The ZnS-SiO<sub>2</sub> (80:20 mol. %) layers (thickness  $d=10$  nm) were deposited at an argon pressure of 0.3 Pa and the intervening a-GST film at 0.4 Pa (as in Ref. 16). For the GST film,  $d$  was chosen to be 60 nm, well beyond the range of screening effects,<sup>27</sup> and within the range used in studies of crystallization-induced stress.<sup>19,28</sup> Power-compensation DSC was performed as in Ref. 16 using a Mettler-Toledo Flash DSC 1,<sup>29</sup> with  $\Phi$  from  $50 \text{ K s}^{-1}$  to  $40\,000 \text{ K s}^{-1}$  under a nitrogen flow of  $20 \text{ ml min}^{-1}$ . As-deposited samples were peeled off the substrates (previous experience including TEM observation suggests that the sandwich structure remains intact) and masses of less than 100 ng were transferred onto the sample area (an Al plate 0.5 mm in diameter) on the chip sensor. DSC traces (Fig. 1) show the exothermic crystallization of a-GST to the metastable fcc phase (confirmed as in Ref. 16), but do not show the glass transition or a transition from fcc to stable hcp. The crystallization exotherms shift to higher  $T_p$  at higher  $\Phi$ . There is some spread in  $T_p$  due to variability in the thermal contact between the samples and the sensor. As in Ref. 16, at any  $\Phi$  most weight is given to the lowest values of  $T_p$  as these reflect the best thermal contact.

The Kissinger plot (Fig. 2) shows the effect of sandwich layers in ultra-fast DSC and in conventional measurements.<sup>10–14</sup> The latter clearly show the inhibition of crystallization as an increased  $T_p$ , this effect being greater for thinner GST films. The ultra-fast DSC data at  $\Phi=50\text{--}1000 \text{ K s}^{-1}$  ( $T_p < 520 \text{ K}$ ) show the same effect, with a trend that can readily be extrapolated through the conventional data. At the highest heating rates ( $\Phi=5000\text{--}40\,000 \text{ K s}^{-1}$ ,  $T_p > 520 \text{ K}$ ),  $T_p$  is lower (crystallization is accelerated) in sandwiched

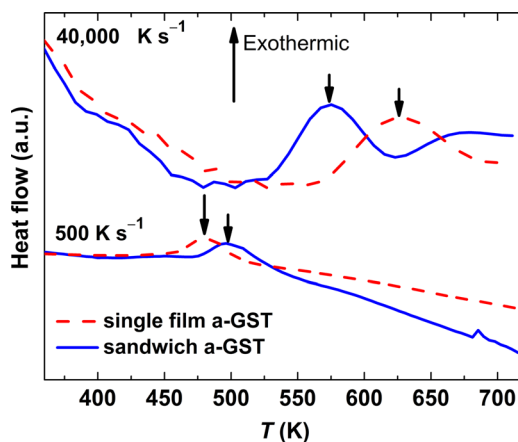


FIG. 1. DSC traces for ultra-fast heating of amorphous GST with and without sandwich layers of ZnS-SiO<sub>2</sub>. Each trace, labelled with the heating rate  $\Phi$ , has an exothermic peak (arrowed at  $T_p$ ) indicating crystallization to the metastable fcc phase. The sandwich structure has two distinct effects: crystallization is impeded at low  $\Phi$  (e.g.,  $500 \text{ K s}^{-1}$ ) but accelerated at high  $\Phi$  (e.g.,  $40\,000 \text{ K s}^{-1}$ ).

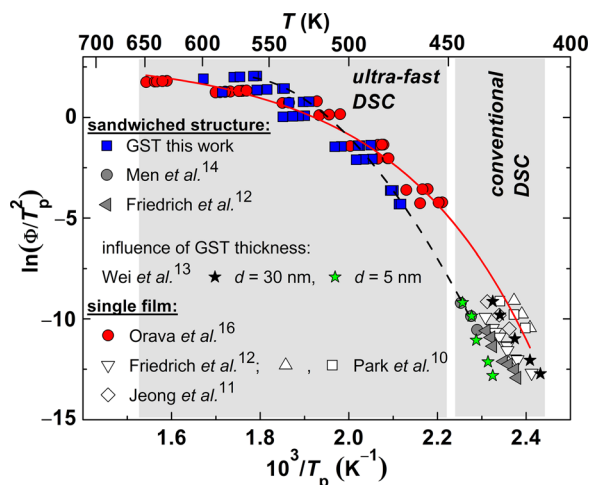


FIG. 2. Kissinger plot comparing crystallization in sandwich structures ZnS-SiO<sub>2</sub>/a-GST/ZnS-SiO<sub>2</sub> with uncapped single-film a-GST. The peak temperature  $T_p$  in DSC, or an analogous crystallization temperature, is measured at different heating rates  $\Phi$ . The data are from Friedrich *et al.* (Ref. 12) (electrical resistometry,  $\Phi = 0.009\text{--}0.09\text{ K s}^{-1}$ , on single films with thickness  $d = 80\text{ nm}$  and sandwich structures with  $d = 4.5/80/4.5\text{ nm}$ ), Wei *et al.* (Ref. 13) (resistometry,  $\Phi = 0.008\text{--}0.33\text{ K s}^{-1}$ ,  $d = 50/5$  or  $30/50\text{ nm}$ ), Men *et al.* (Ref. 14) (optical measurement,  $\Phi = 0.17\text{--}0.67\text{ K s}^{-1}$ ,  $d = 100/20/20\text{ nm}$ ), Park *et al.* (Ref. 10) (conventional DSC,  $\Phi = 0.08\text{--}0.33\text{ K s}^{-1}$ ,  $d = 80\text{ nm}$ ), Jeong *et al.* (Ref. 11) (conventional DSC,  $\Phi = 0.08\text{--}0.33\text{ K s}^{-1}$ ,  $d = 200\text{ nm}$ ), and Orava *et al.* (Ref. 16) (ultra-fast DSC,  $\Phi = 50\text{--}40\,000\text{ K s}^{-1}$ ,  $d = 270\text{ nm}$ ). The shading indicates typical ranges of  $T_p$  for GST observable in conventional and in ultra-fast DSC. The solid red line is the modeling-based fit derived in Ref. 16. The black dashed line is a guide for the eye.

films. Could such a reversal of effect be associated with a change in sign of the hydrostatic stress in the GST film? GST's thermal expansion coefficient is less than that of typical dielectrics,<sup>19</sup> so a film deposited in compression could go into tension on heating. Since crystallization involves shrinkage, such a stress reversal would promote crystallization at lower temperature (heating rate) and inhibit it at higher values. This is the opposite of what is observed, so this explanation of the effects of sandwich layers can be discounted.

In contrast, the inhibition of crystallization at lower temperatures is most easily attributed to stresses induced by the crystallization itself. The shrinkage on crystallization of GST (6.5% in layer thickness) should induce stresses as high as 1.7 GPa in the absence of relaxation,<sup>19</sup> and relaxation is inhibited by capping layers.<sup>28</sup> Crystallization of GST is considered to be nucleation-driven,<sup>15</sup> meaning that internal nucleation is possible, and suggesting that the crystallization should not be subject to surface and interface effects. Yet experiments show that if a free surface is available, crystallization starts there.<sup>5,11,30</sup> As oxygen in GST inhibits crystallization,<sup>31</sup> the free surface is likely favored because stress relaxation is most straightforward there (Fig. 3). It has been suggested<sup>25</sup> and observed<sup>3</sup> that crystallization of confined GST also starts at the interface with the sandwich or capping layers, consistent with such layers having a strong influence on the crystallization.

In the earlier work on uncapped GST films,<sup>16</sup> the Kissinger plot was subjected to a detailed fitting, based on the Cohen and Grest description of the temperature dependence of the liquid viscosity. In the present case, with superposed,

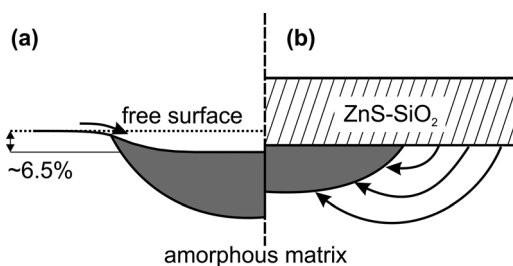


FIG. 3. Schematic half-fields of a crystalline region (shaded) growing at the top surface of a-GST (the shrinkage on crystallization is exaggerated for clarity): (a) at a free surface the shrinkage can be accommodated and there is easy transport by surface diffusion; (b) in contact with a rigid capping layer, the shrinkage can be accommodated only by viscous flow within the amorphous matrix.

temperature-dependent stress effects, such a fitting is not justifiable. Nevertheless, it is possible to compare the temperature dependence of the kinetic coefficient for crystal growth  $U_{\text{kin}}$  with and without sandwich layers. The decoupling of  $U_{\text{kin}}$  from viscosity  $\eta$  as the temperature is lowered towards  $T_g$  can be represented as  $U_{\text{kin}} \propto \eta^{-\xi}$ , where the extent to which  $\xi$  is less than one represents the degree of decoupling.<sup>17</sup> For uncapped GST,  $\xi$  (0.67) fits the correlation with liquid fragility found for oxides and organics<sup>16,17</sup> that may also include metallic glass-forming liquids<sup>32</sup> (Fig. 4). Applying the same analysis as in Ref. 16 to the dashed line in Fig. 2, the effective value of  $\xi$  (0.80) suggests closer coupling (arrow on Fig. 4). The constraint of a capping layer on GST requires viscous flow of the matrix to permit crystal growth (Fig. 3), a coupling effect expected to be greater in thinner films.

In uncapped GST, stresses are low,<sup>19</sup> but their relaxation on heating can be used to estimate the temperature at which viscous flow renders stresses insignificant. By extrapolation, stresses fall to zero at about 500 K,<sup>19</sup> roughly where the data for single and sandwiched films merge (Fig. 2). While heating rate and the differing relaxation rates in the amorphous and crystalline states need to be taken into account, the intersection of the two data sets in Fig. 2 is at least consistent with the conditions for stress relaxation.

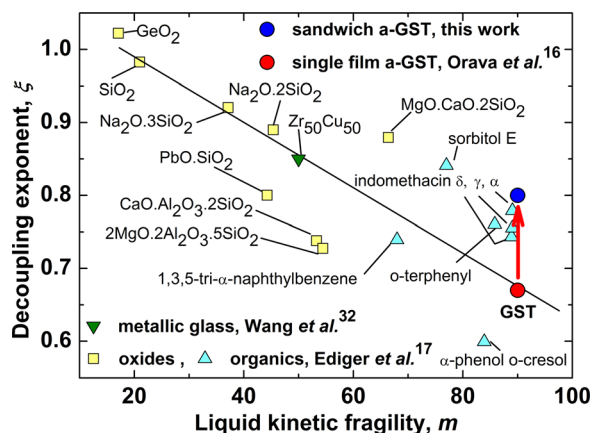


FIG. 4. For a wide variety of glass-forming liquids, the extent of decoupling of crystal growth from viscous flow increases ( $\xi$  decreases) with increasing kinetic fragility  $m$ . Uncapped a-GST fits this correlation (see Ref. 16), but sandwiched films (this work) show closer coupling (arrow).

At still higher  $\Phi$  and  $T_p$ , crystallization is accelerated in sandwiched films. While the discussion has been of dielectric layers impeding crystallization, there are cases of the opposite effect: in optical disks, the CET (governed by crystallization at very high  $\Phi$ ) is shortened if the GST film is in contact with layers of SiC.<sup>15,33</sup> As the temperature is raised, the thermodynamic driving force for crystallization decreases, and for GST above  $\sim 450$  K, this leads to a sharp fall in the calculated rate for homogeneous nucleation of crystals.<sup>34</sup> In that case, heterogeneous nucleation on dielectric layers may be important in promoting crystallization.

We compare the present results with those of Pandian *et al.*<sup>35</sup> on a growth-driven system: (Ge+In)-doped  $Sb_xTe$  thin films with and without sandwich layers. *In-situ* TEM of films isothermally annealed near  $T_g$  showed that the presence of sandwich layers always gives slower growth with a higher  $E_a$ , just as for crystallization of GST (for  $T_p < 520$  K; Fig. 2). Pandian *et al.* conclude that this inhibition of growth, greater at lower temperature, is most reasonably attributed to an effective increase in viscosity due to constraint by the sandwich layers, an argument analogous to that based on coupling in connection with Figs. 3 and 4. Furthermore, they find that while crystal growth is always inhibited by sandwich layers, nucleation can be accelerated.

Recent work on N-doped GST shows that decreasing the cell size in PC-RAM brings benefits in combining faster device switching with greater stability under ambient conditions.<sup>3</sup> With smaller cells, the crystallization of GST is more influenced by extrinsic factors: contact with Ti-W electrodes and the surrounding  $SiO_2$  dielectric. Constraining the GST in a memory cell appears to increase the temperature dependence of the crystallization rate. This is just the effect revealed directly in Fig. 2, where applying sandwich layers does combine inhibition of crystallization at low temperature with acceleration at high temperature.

At low  $\Phi$ , sandwich layers inhibit the crystallization of a-GST, but the Kissinger plot (Fig. 2) shows that this cannot be a good guide to the effects at the higher  $\Phi$  and  $T_p$  relevant for device operation. Although it is still far from the  $10^9$  K  $s^{-1}$  reached in PC-RAM,<sup>13</sup> the great range of  $\Phi$  possible with ultra-fast DSC does permit study of crystallization over a temperature range sufficient to interpret device operation. The inhibition of crystallization, a stronger effect in thinner films, is attributed to crystallization-induced stress strengthening the coupling between crystal growth and viscous flow. The effect disappears at higher temperature, consistent with the kinetics of stress relaxation. At higher  $\Phi$  and  $T_p$ , the data suggest that sandwich layers can catalyze crystallization. Ultra-fast DSC shows that constraint by the layers increases the temperature dependence of crystallization in GST. This effect is certainly beneficial for device performance and will be of increasing importance as memory cells continue to decrease in size. Further work, exploring the effects of film thickness and of different sandwich layers representative of the electrode and dielectric materials in PC-RAM, should be useful in improving device reliability and scalability.

J.O., A.L.G., B.G., and D.W.H. acknowledge support from the Engineering and Physical Sciences Research Council (UK), B.G. and D.W.H. in part through the EPSRC Centre for Innovative Manufacturing in Photonics.

- <sup>1</sup>M. Wuttig and N. Yamada, *Nature Mater.* **6**, 824 (2007).
- <sup>2</sup>G. W. Burr, M. J. Breitwisch, M. Franceschini, D. Garetto, K. Gopalakrishnan, B. Jackson, B. Kurdi, C. Lam, L. A. Lastras, A. Padilla, B. Rajendran, S. Raoux, and R. S. Shenoy, *J. Vac. Sci. Technol. B* **28**, 223 (2010).
- <sup>3</sup>W. Wang, D. Loke, L. Shi, R. Zhao, H. Yang, L.-T. Law, L.-T. Ng, K.-G. Lim, Y.-C. Yeo, T.-C. Chong, and A. L. Lacaita, *Sci. Repts.* **2**, 360 (2012).
- <sup>4</sup>M. Wuttig and M. Salinga, *Nature Mater.* **11**, 270 (2012).
- <sup>5</sup>B. J. Kooi, W. M. G. Groot, and J. Th. M. De Hosson, *J. Appl. Phys.* **95**, 924 (2004).
- <sup>6</sup>S. Privitera, C. Bongiorno, E. Rimini, and R. Zonca, *Appl. Phys. Lett.* **84**, 4448 (2004).
- <sup>7</sup>J. Kalb, F. Spaepen, and M. Wuttig, *Appl. Phys. Lett.* **84**, 5240 (2004).
- <sup>8</sup>T. H. Lee and S. R. Elliott, *Phys. Rev. Lett.* **107**, 145702 (2011).
- <sup>9</sup>H. E. Kissinger, *Anal. Chem.* **29**, 1702 (1957).
- <sup>10</sup>J. Park, M. R. Kim, W. S. Choi, H. Seo, and C. Yeon, *Jpn. J. Appl. Phys., Part 1* **38**, 4775 (1999).
- <sup>11</sup>T. H. Jeong, M. R. Kim, H. Seo, S. J. Kim, and S. Y. Kim, *J. Appl. Phys.* **86**, 774 (1999).
- <sup>12</sup>I. Friedrich, V. Weidenhof, W. Njoroge, P. Franz, and M. Wuttig, *J. Appl. Phys.* **87**, 4130 (2000).
- <sup>13</sup>X. Wei, L. Shi, T. C. Chong, R. Zhao, and H. K. Lee, *Jpn. J. Appl. Phys., Part 1* **46**, 2211 (2007).
- <sup>14</sup>L. Men, J. Tominaga, H. Fuji, T. Kikukawa, and N. Atoda, *Jpn. J. Appl. Phys., Part 1* **40**, 1629 (2001).
- <sup>15</sup>G.-F. Zhou, *Mater. Sci. Eng. A* **304–306**, 73 (2001).
- <sup>16</sup>J. Orava, A. L. Greer, B. Gholipour, D. W. Hewak, and C. E. Smith, *Nature Mater.* **11**, 279 (2012).
- <sup>17</sup>M. D. Ediger, P. Harrowell, and L. Yu, *J. Chem. Phys.* **128**, 034709 (2008).
- <sup>18</sup>N. Ohshima, *J. Appl. Phys.* **79**, 8357 (1996).
- <sup>19</sup>T. P. Leervad Pedersen, J. Kalb, W. K. Njoroge, D. Wamwangi, M. Wuttig, and F. Spaepen, *Appl. Phys. Lett.* **79**, 3597 (2001).
- <sup>20</sup>H.-Y. Cheng, S. Raoux, and Y.-C. Chen, *J. Appl. Phys.* **107**, 074308 (2010).
- <sup>21</sup>S. Raoux, J. L. Jordan-Sweet, and A. J. Kellock, *J. Appl. Phys.* **103**, 114310 (2008).
- <sup>22</sup>R. E. Simpson, M. Krbal, P. Fons, A. V. Kolobov, J. Tominaga, T. Uruga, and H. Tanida, *Nano Lett.* **10**, 414 (2010).
- <sup>23</sup>S. Song, Z. Song, L. Wu, B. Liu, and S. Feng, *J. Appl. Phys.* **109**, 034503 (2011).
- <sup>24</sup>Z. Fan and D. E. Laughlin, *Jpn. J. Appl. Phys., Part 1* **42**, 800 (2003).
- <sup>25</sup>S. Raoux, H.-Y. Cheng, J. L. Jordan-Sweet, B. Muñoz, and M. Hitzbleck, *Appl. Phys. Lett.* **94**, 183114 (2009).
- <sup>26</sup>M. Zacharias, J. Bläsing, P. Velt, L. Tsybeskov, K. Hirschman, and P. M. Fauchet, *Appl. Phys. Lett.* **74**, 2614 (1999).
- <sup>27</sup>M. Zacharias and P. Streitenberger, *Phys. Rev. B* **62**, 8391 (2000).
- <sup>28</sup>Q. Guo, M. Li, Y. Li, L. Shi, T. C. Chong, J. A. Kalb, and C. V. Thompson, *Appl. Phys. Lett.* **93**, 221907 (2008).
- <sup>29</sup>V. Mathot, M. Pyda, T. Pijpers, G. Vanden Poel, E. van de Kerkhof, S. van Herwaarden, F. van Herwaarden, and A. Leenaers, *Thermochim. Acta* **522**, 36 (2011).
- <sup>30</sup>S. H. Lee, Y. Jung, and R. Agarwal, *Nano Lett.* **8**, 3303 (2008).
- <sup>31</sup>S. Privitera, E. Rimini, and R. Zonca, *Appl. Phys. Lett.* **85**, 3044 (2004).
- <sup>32</sup>Q. Wang, L.-M. Wang, M. Z. Ma, S. Binder, T. Volkman, D. M. Herlach, J. S. Wang, Q. G. Xue, Y. J. Tian, and R. P. Liu, *Phys. Rev. B* **83**, 014202 (2011).
- <sup>33</sup>G.-F. Zhou and B. A. J. Jacobs, *Jpn. J. Appl. Phys., Part 1* **38**, 1625 (1999).
- <sup>34</sup>U. Russo, D. Ielmini, and A. L. Lacaita, *IEEE Trans. Electron Devices* **54**, 2769 (2007).
- <sup>35</sup>R. Pandian, B. J. Kooi, J. Th. M. De Hosson, and A. Pauza, *J. Appl. Phys.* **100**, 123511 (2006).